Chapter IV Modeling of the Association Behavior of Linear Chains with Strongly Associating Endgroups

4.1 Introduction

Our work so far has investigated whether linear chains possessing associating functional groups grafted at random positions along the entire chains can be useful as mist-control additives to aviation fuel. Molecular designs involving both self-associating interactions and donor-acceptor interactions were studied, and the effects of extent of functionalization as well as concentration of polymer components on shear and extensional rheology of dilute solutions in non-polar hydrocarbon solvents were examined. We have found that for both self-associating and donor-acceptor systems, intra- and intermolecular associations cause collapse of the chains and interfere with the mechanism of mist control by inhibiting stretching of the chain in extentional flow. In this chapter, we consider molecular designs that overcome chain collapse by clustering associating groups at the ends of polymer chains. In particular, we construct a model that predicts, for long linear chains endcapped with strongly associating A and B groups, the equilibrium partitioning of the polymer into supramolecular linear chains and supramolecular loops of all sizes (Scheme 4.1). We assume that the A and B endgroups associate with each other pair-wise with interaction energy εkT, but that neither the A nor the B endgroups self-associate.

4.2 Theoretical

To model the equilibrium aggregation of telechelic polymers A----A and B----B into supramolecular cyclic and linear chains of any length (Scheme 4.1), we consider the simpler case of association of telechelic polymers A_1----A_2 and B_1----B_2, and argue that results are the same (Section 4.2.6). In doing so, we assume that the end-groups A_1 and A_2, and likewise B_1 and B_2, are distinguishable but of identical reactivity (as might be the case, for example, if one atom of A_1 were a different isotope than the corresponding atom of A_2). What is the equilibrium distribution of all the aggregates for a given energy of association εkT? We can estimate this equilibrium assuming ideal solutions by making use of the following lattice model.[1]

4.2.1 Model Description

Consider a solution composed of N_s solvent molecules and N_{Atotal} and N_{Btotal} telechelic A_1----A_2 and B_1----B_2 chains, of respective length M_A and M_B elementary units (monomers). The solution volume V is partitioned into lattice sites of volume a^3, where a^3 is the volume of a solvent molecule and also the volume of a monomer. We will assume that there is no volume change upon mixing, so that $V = a^3(N_s + N_{Atotal}M_A + N_{Btotal}M_B) = \Lambda a^3$, where Λ is the total number of "sites." We will use the subscript s to refer to the solvent and the subscripts i or j to refer to single-chain and supramolecular components. Unless otherwise specified, sums $\sum_j$ are over all polymer components in solution, i.e., the telechelic starting materials and all polymer aggregates. The volume fractions of solvent and polymer component j are $\phi_s = N_s/\Lambda$ and $\phi_j = N_jM_j/\Lambda$, where M_j is the number of monomers of polymer component j. Let $\phi = \sum_j M_jN_j/\Lambda = 1-\phi_s$ denote the total polymer volume fraction in solution. The center-of-mass and configurational entropy of the polymer components and solvent is:

$$S = k\sum_j \ln \Omega(0, N_j) + \Delta S_{mix} \tag{4.1}$$

where $\Omega(0,N_j)$ is the number of possible configurations of N_j molecules of polymer component j, each of length M_j, onto M_jN_j sites (referring to pure polymer before mixing), so that the sum accounts for the entropy of all the polymer components before mixing. Here we have retained the notation of Hill[2] for the entropy of a pure solution of N_i linear polymer chains of length M_i:

$$\ln \Omega(0, N_i) = -N_i \ln N_i + N_i + M_iN_i \ln(M_iN_i) - M_iN_i + N_i(M_i - 1)\ln\left(\frac{c-1}{M_iN_i}\right) \tag{4.2}$$

where c is the coordination number, i.e., the number of sites neighboring any given monomer where the next monomer on the chain may be found. The entropy of mixing of the solvent and all polymer components, $\Delta S_{mix,}$ is approximated using the Flory-Huggins expression:

$$\Delta S_{mix} = -k\left(N_s \ln \phi_s + \sum_j N_j \ln \phi_j\right). \tag{4.3}$$

Equation 4.1 does not account for the entropic cost of loop closure for supramolecular cycles; that contribution will instead be absorbed into the standard chemical potential of the cyclic components, as discussed later. The entropic contribution to the mixture's free energy is therefore:

$$\begin{aligned} F_S &= -T\Delta S_{mix} - kT\sum_j \ln\Omega(0,N_j) \\ &= kT\left[N_s \ln\left(\frac{N_s}{\Omega}\right) + \sum_j N_j \ln\left(\frac{N_j}{\Omega}\right)\right] + kT\sum_j N_j \ln\left(M_j\right) - kT\sum_j \ln\Omega(0,N_j). \end{aligned} \tag{4.4}$$

Next, the contribution to the solution free energy due to solvent-solvent, polymer-solvent, and polymer-polymer interactions is estimated by the random mixing approximation:

$$F_{int} = \Omega\delta\left[(1-\phi)^2 h_{ss} + \phi^2 h_{pp} + 2\phi(1-\phi)h_{ps}\right] \tag{4.5}$$

where δ is one-half the local coordination number, and h_{ij} are the microscopic interaction energies of the polymer and solvent species. The total free energy F of the solution is the sum of F_S, F_{int}, and of contributions from the internal free energy of solvent and polymer components:

$$F = F_{int} + F_S + N_s\mu_s^0 + \sum_j N_j\mu_j^0 \tag{4.6}$$

where μ_i^0 is the standard chemical potential of the single-chain or supramolecular chain component i. Using $\phi = (M_iN_i + \sum_{j\neq i} M_jN_j)/\Lambda$ with $\Lambda = N_s + M_iN_i + \sum_{j\neq i} M_jN_j$, the contribution to the chemical potential of polymer component i due to interactions is:

$$\mu_{int,i} = \left.\frac{\partial F_{int}}{\partial N_i}\right|_{N_{j\neq i}} = -\omega M_i\phi_s^2 + \omega_{pp}M_i \tag{4.7}$$

where for convenience we have introduced $\omega_{mn} = \delta h_{mn}$ and $\omega = \omega_{pp} + \omega_{ss} - 2\,\omega_{ps}$. The entropic contribution to the chemical potential of polymer component i is:

$$\begin{aligned} \frac{\mu_{S,i}}{kT} = \frac{1}{kT}\left.\frac{\partial F_S}{\partial N_i}\right|_{N_{j\neq i}} &= \ln\left(\frac{\phi_i}{M_i}\right) + 1 - \phi_i - M_i\left[\phi_s + \sum_{j\neq i}\frac{\phi_j}{M_j}\right] + \ln M_i \\ &\quad -1 - M_i\left[\ln(c-1) - 1\right] - \ln M_i + \ln(c-1) \end{aligned} \tag{4.8}$$

or, after rearranging:

$$\frac{1}{kT}\left.\frac{\partial F_S}{\partial N_i}\right|_{N_{j\neq i}} = \ln\left(\frac{\phi_i}{M_i}\right) - M_i\left[\phi_s + \sum_j \frac{\phi_j}{M_j}\right] + f_i \tag{4.9}$$

where f_i = ln(c-1) + M_i[1-ln(c-1)]. Differentiation of Equation 4.6 and substitution of Equations 4.7 and 4.9 give the following expression for the chemical potential of component i, valid for the single-chain building blocks and all aggregates:

$$\mu_i = \left.\frac{\partial F}{\partial N_i}\right|_{N_{j\neq i}} = \mu_i^0 + kT\left\{\ln\left(\frac{\phi_i}{M_i}\right) - M_i\left[\phi_s + \sum_j \frac{\phi_j}{M_j}\right] + f_i\right\} - \omega M_i \phi_s^2 + \omega_{pp} M_i . \quad (4.10)$$

Consider a supramolecular component i made up of n_i A_1----A_2 building blocks and m_i B_1----B_2 building blocks: its size is $M_i = n_i M_A + m_i M_B$. At the equilibrium partitioning of the telechelic building blocks into aggregates of all size, its chemical potential satisfies the equilibrium condition:

$$\mu_i = n_i \mu_A + m_i \mu_B \quad (4.11)$$

where μ_A and μ_B are the chemical potentials of building blocks A_1----A_2 and B_1----B_2, respectively. Substituting the expressions for μ_i, μ_A, and μ_B from Equation 4.10 into Equation 4.11 above, we obtain, after rearrangement, the following mass-action relation for polymer component i:

$$\mu_i^0 + kT\left[\ln\left(\frac{\phi_i}{M_i}\right) + f_i\right] = n_i\mu_A^0 + m_i\mu_B^0 + kT\left[n_i \ln\left(\frac{\phi_A}{M_A}\right) + m_i \ln\left(\frac{\phi_B}{M_B}\right) + n_i f_A + m_i f_B\right] \quad (4.12)$$

where ϕ_A, ϕ_B are the volume fractions of the telechelic building blocks A_1----A_2 and B_1----B_2, respectively. Equation 4.12 above can be rewritten as follows:

$$\left(\frac{\phi_i}{n_i M_A + m_i M_B}\right) = \left(\frac{\phi_A}{M_A}\right)^{n_i}\left(\frac{\phi_B}{M_B}\right)^{m_i} \exp(\Gamma_i) \quad (4.13)$$

where
$$\Gamma_i = \frac{1}{kT}(n_i\mu_A^0 + m_i\mu_B^0 - \mu_i^0) + (n_i + m_i - 1)\ln(c-1). \quad (4.14)$$

The conservation equations are then:

$$\begin{aligned}
\phi_{Atotal} &= \sum_j \phi_j \left(\frac{n_j M_A}{n_j M_A + m_j M_B}\right) = \sum_j n_j M_A \left(\frac{\phi_A}{M_A}\right)^{n_j}\left(\frac{\phi_B}{M_B}\right)^{m_j} \exp(\Gamma_j) \\
\phi_{Btotal} &= \sum_j \phi_j \left(\frac{m_j M_B}{n_j M_A + m_j M_B}\right) = \sum_j m_j M_B \left(\frac{\phi_A}{M_A}\right)^{n_j}\left(\frac{\phi_B}{M_B}\right)^{m_j} \exp(\Gamma_j).
\end{aligned} \quad (4.15)$$

In our construction of the model, terms arising from microscopic interactions, as well as terms arising from the center-of-mass and configurational entropy (except loop closure) of polymer components and solvent in solution have been carried out explicitly. On the other hand, terms arising from (i) the energy of association of the endgroups within a polymer aggregate, and (ii) the entropic cost of loop closure for cyclic supramolecular aggregates, are instead absorbed into the standard chemical potentials μ_j^0 of the aggregates. We now proceed to derive expressions accounting for these effects.

4.2.2 Entropic Cost of Loop Closure

The entropic cost of loop closure is determined by calculating the probability of loop closure, as follows: For Gaussian linear chains of N Kuhn monomers of length b, the probability density function for the end-to-end vector $\mathbf{r}$ is:[3]

$$G_{Gaussian}(\mathbf{r},N)=\left(\frac{3}{2\pi Nb^2}\right)^{\frac{3}{2}}\exp\left\{-\frac{3\mathbf{r}^2}{2Nb^2}\right\}. \tag{4.16}$$

The argument within the exponential is $-3\mathbf{r}^2/(2Nb^2) \cong 0$ for $\|\mathbf{r}\| << \langle\mathbf{r}^2\rangle^{1/2}$, so the probability that the chain ends be within a small distance x of each other, where $x/b \sim O(1)$, is:

$$\begin{aligned} G_{cyc,Gaussian} &= \left(\frac{3}{2\pi Nb^2}\right)^{\frac{3}{2}}\int_0^{2\pi}d\phi\int_0^{\pi}d\theta\sin\theta\int_0^{a}dr\cdot r^2\exp(0) \\ &= 4\pi\left(\frac{3}{2\pi Nb^2}\right)^{\frac{3}{2}}\int_0^{a}dr\cdot r^2\exp(0)=\left(\frac{6}{\pi N^3}\right)^{\frac{1}{2}}\left(\frac{x}{b}\right)^3. \end{aligned} \tag{4.17}$$

For real chains, excluded volume interactions of the monomers at chain ends reduce the probability density function $G(\mathbf{r},N)$ by the factor

$$\frac{G_{real}(\mathbf{r},N)}{G_{Gaussian}(\mathbf{r},N)}\sim\left(\frac{\|\mathbf{r}\|}{\sqrt{\langle\mathbf{r}^2\rangle}}\right)^g \qquad \text{for } \frac{\|\mathbf{r}\|}{\sqrt{\langle\mathbf{r}^2\rangle}}<<1 \tag{4.18}$$

where the exponent $g \cong 0.28$,[4] so that the probability of cyclization becomes

$$G_{cyc,real}\approx 4\pi\left(\frac{3}{2\pi Nb^2}\right)^{\frac{3}{2}}\left(\frac{1}{bN^{\nu}}\right)^g\int_0^{a}dr\cdot r^{2+g}\exp(0)\sim N^{-3/2-g\nu} \tag{4.19}$$

where the fractal exponent ν is 0.588 in good solvent. The loop closure probability thus scales as $N^{-3/2}$ for Gaussian chains and $N^{-1.66}$ for swollen chains. The entropic cost of loop closure is simply $\Delta S_{loop} = -k\ln G_{cyc}$.

In dilute or semi-dilute solutions, all chain segments smaller than the thermal blob $g_T \approx b^6/v^2$ (where v is the excluded volume parameter) have nearly Gaussian statistics because excluded volume interactions are weaker than the thermal energy. If, for our solution composed of any number of different (single and supramolecular) chains j of size M_j, at total polymer volume fraction $\phi = \sum_j \phi_j$, we assume that the polymer chains are dilute enough to ignore polymer-polymer interactions, we can use the following expression in the calculation of the entropic cost of loop closure $\Delta S_{loop} = -k\ln G_{cyc}$ for any cyclic aggregate q:

$$G_{cyc,q} \approx \left(\frac{6}{\pi g_T^3}\right)^{\frac{1}{2}} \left(\frac{x}{b}\right)^3 \left(\frac{M_q}{g_T}\right)^{-1.66} . \tag{4.20}$$

By doing so we are simply assuming that all chain segments larger than g_T are fully swollen.

4.2.3 Inventory of Polymer Components

As a starting point in classifying the polymer aggregates, we group them together as shown in Figure 4.1. Let index g refer to groups, and ϕ_g refer to the cumulative volume fraction of all the polymer components that belong to group g. All the polymer components j that belong to any particular group g have the same values of $M_j = M_g$, $n_j = n_g$, $m_j = m_g$, and $\Gamma_j = \Gamma_g$, so the equilibrium condition and the conservation equations can be rewritten as:

$$\left(\frac{\phi_g}{n_g M_g + m_g M_g}\right) = \Omega_g \left(\frac{\phi_A}{M_A}\right)^{n_g} \left(\frac{\phi_B}{M_B}\right)^{m_g} \exp(\Gamma_g) \tag{4.21}$$

$$\begin{aligned} \phi_{Atotal} &= \sum_g n_g M_A \Omega_g \left(\frac{\phi_A}{M_A}\right)^{n_g} \left(\frac{\phi_B}{M_B}\right)^{m_g} \exp(\Gamma_g) \\ \phi_{Btotal} &= \sum_g m_g M_B \Omega_g \left(\frac{\phi_A}{M_A}\right)^{n_g} \left(\frac{\phi_B}{M_B}\right)^{m_g} \exp(\Gamma_g) \end{aligned} \tag{4.22}$$

where Ω_g refers to the number of distinct species in group g.

How many components belong to each group? For linear aggregates there are two possibilities: (i) if $n_g + m_g$ is even (i.e., $n_g = m_g$), then no sequence read from left to right will

be the same as a sequence read from right to left, so the number of ways to arrange the molecules is $\Omega_g = 2^{n_g+m_g}$; (ii) if $n_g + m_g$ is odd, then every sequence read from left to right will have a matching sequence read from right to left, so the number of ways to arrange the molecules is $\Omega_g = 2^{n_g+m_g-1}$. Supramolecular cycles can only be formed if $n_g = m_g$. The number of ways to form such a loop is derived below; to a very good approximation it is $\Omega_{cyc,g} = 2 + (2^{2n_g-1} - 2)/n_g$.

4.2.4 Number of Ways to Form Loops

We seek to determine the number of different loops that can be formed by linking n A_1----A_2 and n B_1----B_2 telechelic chains end-to-end via association of A and B endgroups, as shown in Figure 4.2 (left). We are assuming that A_1 groups are distinguishable from A_2 groups, and likewise B_1 groups are distinguishable from B_2 groups, but that the n A_1----A_2 molecules are indistinguishable, and likewise are the n B_1----B_2 molecules. The question is equivalent to the combinatorial problem of counting necklaces formed using beads of different colors, in which two necklaces are considered equivalent if one can be rotated to give the other. The way to recognize the equivalence is to break up the loops into adjacent pairs of telechelics (with one A_1----A_2 and one B_1----B_2 molecule per pair), and map the loops into necklaces made up of n beads of 4 different colors as shown in Figure 4.2. The formula for the number of different necklaces is:[5]

$$m(n) = \frac{1}{n}\sum_{d|n}\left[\varphi(d)\cdot 4^{n/d}\right] \tag{4.23}$$

where the sum is over all numbers d that divide n, and $\varphi(d)$ is the Euler phi function.

In reality, the above formula overcounts the number of ways to form polymer loops by a factor of 2. To see this, observe that any loop can be "read" in two ways (clockwise and counter-clockwise) to give two *distinct* necklaces. This is true because we cannot create an arbitrary loop which can be "read" the same clockwise and counterclockwise, no matter where we begin to read (Figure 4.3). Consider now the $m(n)$ distinct necklaces obtained from n beads, and the $s(n)$ distinct loops obtained from n A_1----A_2 and n B_1----B_2 telechelic chains, forming sets $\{\text{necklaces}_n\}$ and $\{\text{loops}_n\}$. Each necklace in $\{\text{necklaces}_n\}$ uniquely maps into a polymer loop in the set $\{\text{loops}_n\}$, but every loop in $\{\text{loops}_n\}$ maps back to two different necklaces, which must belong to $\{\text{necklaces}_n\}$. The elements of $\{\text{necklaces}_n\}$ can therefore

be arranged pairwise as shown in Figure 4.4, revealing that there are twice as many elements in {necklaces$_n$} than in {loops$_n$}. The number of distinct loops $s(n)$ that can be formed by linking n A_1----A_2 and n B_1----B_2 telechelic chains end-to-end via association of A and B endgroups is therefore:

$$s(n) = \frac{1}{2n}\sum_{d|n}\left[\varphi(d)\cdot 4^{n/d}\right]. \tag{4.24}$$

4.2.5 Standard Chemical Potential of Polymer Aggregates

In Equations 4.13–4.15 and 4.21–4.22, we chose to absorb into the expressions for the standard chemical potential of the aggregates μ_j^0 the contributions due to the energy of association of the endgroups and to the entropic cost of loop closure. The equation for the standard chemical potential of any polymer component j within group g is therefore:

$$\mu_g^0 = \begin{cases} n_g\mu_A^0 + m_g\mu_B^0 - \varepsilon kT(n_g+m_g) - kT\ln G_{cycl,g} & \text{if cyclic} \\ n_g\mu_A^0 + m_g\mu_B^0 - \varepsilon kT(n_g+m_g-1) & \text{if linear,} \end{cases} \tag{4.25}$$

so that Γ_g in the equilibrium and conservation relationships (Equation 4.21 and 4.22) is:

$$\Gamma_g = \begin{cases} \varepsilon(n_g+m_i) + (n_i+m_i-1)\ln(c-1) + \ln G_{cycl,g} & \text{if cyclic} \\ \varepsilon(n_g+m_g-1) + (n_g+m_g-1)\ln(c-1) & \text{if linear.} \end{cases} \tag{4.26}$$

4.2.6 Distinguishable versus Indistinguishable Endgroups

Consider the reversible association reactions shown in Scheme 4.2 (endgroups are indistinguishable in case b, but distinguishable in c). In each of cases a, b, and c, let ϕ_A and ϕ_B be the volume fractions of the starting materials, and ϕ_{dimer} be the total volume fraction of product dimers. For the product in case a and each of the products in case c, the equilibrium condition (Equation 4.13) is the same:

$$\left(\frac{\phi_{dimer}}{M_A+M_B}\right) = \left(\frac{\phi_A}{M_A}\right)\left(\frac{\phi_B}{M_B}\right)\exp(\Gamma) \qquad \text{in case a} \tag{4.27}$$

and

$$\left(\frac{\tfrac{1}{4}\phi_{dimer}}{M_A+M_B}\right) = \left(\frac{\phi_A}{M_A}\right)\left(\frac{\phi_B}{M_B}\right)\exp(\Gamma) \qquad \text{in case c} \tag{4.28}$$

where M_A and M_B are the number of monomers in the starting materials, and $\Gamma = \varepsilon + \ln(c\text{-}1)$ according to Equation 4.26. In Equation 4.28, ¼ ϕ_{dimer} is the volume fraction of each of the product dimers, so the difference in Equations 4.27 and 4.28 simply reflects the difference in the number of ways to form dimers, i.e., $\Omega_c = 4$ while $\Omega_a = 1$. The correspondingly larger equilibrium fraction of dimers in case c can be intuitively understood to be a mere consequence of the increased contact probability of the endgroups to form the product: the rate of dissociation of dimers is equal in both cases, but the rate of association of reactants is expected to be 4 times greater in case b.

What is the equilibrium condition for the total volume fraction of product dimers in case b? If the endgroups A, A_1, and A_2 have precisely the same reactivity, and likewise the endgroups B, B_1, and B_2, there cannot be any difference in the equilibrium partitioning of the molecules in cases b and case c, so that the equilibrium condition for case b is Equation 4.28, not Equation 4.27. We generalize this argument to conclude that the solution to the equilibrium problem presented in Scheme 4.1, where endgroups are indistinguishable, is expected to be that solution which we developed for telechelics A_1----A_2 and B_1----B_2, where endgroups are distinguishable. A less careful modeling of the association of telechelic polymers A----A and B----B might miscalculate the cumulative equilibrium volume fraction of polymer aggregates that fall within any group g by omitting the factor Ω_g in Equation 4.21.

4.2.7 Addition of End-Capping Chains

Addition of "end-capping chains" can be used to alter the relative partitioning into linear vs. cyclic aggregates, and the model can be extended to capture that behavior. Consider the addition of $N_{captotal}$ end-capping A---- chains, of length M_{cap} and total volume fraction $\phi_{captotal}$. Let $p_j = p_g$ refer to the number of end-capping A---- chains in any polymer component j belonging to group g and let ϕ_{cap} be the equilibrium volume fraction of free A---- chains. The equilibrium condition for any group g becomes:

$$\left(\frac{\phi_g}{n_g M_A + m_g M_B + p_g M_{cap}}\right) = \Omega_g \left(\frac{\phi_A}{M_A}\right)^{n_g} \left(\frac{\phi_B}{M_B}\right)^{m_g} \left(\frac{\phi_{cap}}{M_{cap}}\right)^{p_g} \exp(\Gamma_g) \qquad (4.29)$$

with
$$\Gamma_g = \begin{cases} \varepsilon(n_g + m_g) + (n_g + m_g - 1)\ln(c-1) + \ln G_{cycl,g} & \text{if cyclic} \\ (n_g + m_g + p_g - 1)\left[\varepsilon + \ln(c-1)\right] & \text{if linear} \end{cases} \qquad (4.30)$$

where for endcapped aggregates $\Omega_{cap,g} = 2^{n_g+m_g} / p_g$, and the expressions for Ω_g for cyclic and non-endcapped linear aggregates are given in Section 4.2.3. The conservation equations become:

$$\begin{aligned}
\phi_{Atotal} &= \sum_g n_g M_A \Omega_g \left(\frac{\phi_A}{M_A}\right)^{n_g} \left(\frac{\phi_B}{M_B}\right)^{m_g} \left(\frac{\phi_{cap}}{M_{cap}}\right)^{p_g} \exp(\Gamma_g) \\
\phi_{Btotal} &= \sum_g m_g M_B \Omega_g \left(\frac{\phi_A}{M_A}\right)^{n_g} \left(\frac{\phi_B}{M_B}\right)^{m_g} \left(\frac{\phi_{cap}}{M_{cap}}\right)^{p_g} \exp(\Gamma_g) \\
\phi_{captotal} &= \sum_g p_g M_{cap} \Omega_g \left(\frac{\phi_A}{M_A}\right)^{n_g} \left(\frac{\phi_B}{M_B}\right)^{m_g} \left(\frac{\phi_{cap}}{M_{cap}}\right)^{p_g} \exp(\Gamma_g).
\end{aligned} \tag{4.31}$$

4.3 Computational

We want to test whether linear chains possessing strongly associating endgroups can be useful as mist-control additives to aviation fuel. In the present chapter, computational results are given for a case of practical significance that can be tested experimentally using anionically polymerized telechelics: monodisperse polyisoprene (PI) chains with strongly associating endgroups, in dilute solutions in Jet-A solvent. We will address the nature of the endgroups in Section 4.5.6.

4.3.1 Choice of Parameters

The model has assumed that solvent molecules and polymer elementary units have the same size a^3. In general, we cannot expect that to be the case. If the volume of a solvent molecule (v_s) differs from that of a monomer, how should we choose the lattice size a, and how many lattice sites M should be assigned to a polymer chain of molecular weight MW_p?

We want to model a mixture of N_s solvent molecules and N_p monodisperse polymer chains of molecular weight MW_p. If we wish to preserve the volume fraction and number densities of polymer and solvent molecules, then we require that $N_s a^3 = N_s v_s$ and $N_p M a^3 = N_p(MW_p/MW_o)v_{mon}$, where v_{mon} and MW_o are the volume and molecular weight of a chemical monomer. These conditions require that $a^3 = v_s$ and $M = (MW_p/MW_o)\ (v_{mon}/a^3)$, meaning that the number and size of the elementary units into which we break up the chains is determined by the solvent size v_s. In this way, we have sacrificed the freedom to map the polymer chain as we might otherwise wish to: for instance, use of Equations 4.16–4.20 assumes that the

polymer chain has been mapped into an equivalent freely jointed chain with $M = MW_p/MW_K$ Kuhn monomers, where MW_K is the molecular weight of a Kuhn momomer.

An alternative is to model a solution of N_p monodisperse polymer molecules of given number density N_p/V and volume fraction ϕ_p. This method lets the monomer size determine the lattice size and renormalizes the number of solvent molecules, as follows. Preserving the polymer volume fraction and number density requires that $N_{s,model}a^3 = N_{s,real}v_s$ and $N_pMa^3 = N_p(MW_p/MW_o)v_{mon}$, where $N_{s,real}$ and $N_{s,model}$ are the number of real and model solvent molecules dissolving the polymer chains, and other parameters are the same as above. In this manner we are free to map the polymer chains in whatever way we choose to. The cost of that improvement is that the number density of the solvent molecules is not preserved, but since that number does not appear in the equilibrium equations (Equation 4.13–4.14), it seems inconsequential.

In what follows, we have adopted the latter approach and chosen to break up the chain into $M = MW_p/MW_K$ Kuhn monomers using $a^3 = v_{mon}MW_K/MW_o = v_K$, where v_K is the volume of a Kuhn monomer, and $N_{s,model} = N_{s,real}v_s/v_K$.

4.3.2 Parameter Values

We are choosing to break-up the polymer into Kuhn monomers of molecular weight MW_K, and to set the lattice size as $a^3 = v_K = MW_K/(\mathcal{N}_A\rho)$, where $\mathcal{N}_A$ is Avogadro's constant and ρ is the polymer density. For 1,4-PI polymer,[6] $\rho = 0.83$ g/cm^3 and $MW_K = 113$ g/mol, giving $a \approx 6.1$ Å. To quantitate the entropic cost of loop closure, numerical values are needed for the end-to-end distance x we require to close the loop and for the number of monomers in a thermal blob $g_T \approx b^6/v^2$. For simplicity we arbitrarily choose $x/b = 1$. The excluded volume parameter v was estimated[7] to be such that $v/b^3 \approx 0.10$ for PI in Jet-A, giving $g_T \approx 100$. Finally, we assume that the random walks of the chains on the lattice correspond to a coordination number of $c = 6$.

4.3.3 Computations

The following procedure was used to calculate the volume fraction of all polymer components (i.e., single-chain starting materials and aggregates of all sizes) at equilibrium, for polymer solutions of A_1----A_2 and B_1----B_2 telechelics and A---- "end-cap" chains of

specified molecular weights at specified initial concentrations ϕ_{Atotal}, ϕ_{Btotal}, and $\phi_{captotal}$ (polymer components were grouped as shown in Figure 4.5):

- First, choose a number of groups T_{groups} to include in the analysis (even though there is an infinite number of possible polymer components, we expect that above a certain size, polymer aggregates will have negligible equilibrium volume fraction and can therefore be ignored)
- Calculate n_g, m_g, M_g, Ω_g, $G_{cyc,g}$ (if appropriate), and Γ_g for polymer group g, for g = 1… T_{groups}
- Solve the three conservation equations, Equations 4.31, for (ϕ_A, ϕ_B, ϕ_{cap})
- Calculate ϕ_g for g = 1… T_{groups} using Equation 4.29
- Repeat with a new value of T_{groups} twice that of the previous one until changes in the calculated values of ϕ_g from one value of T_{groups} to the next are negligible.

4.4 Results

To translate model results into terms relevant to experiment, the equilibrium distribution of aggregates is described in terms of the concentration of the various size supramolecular species. In the context of polymer-induced mist-suppression, all linear aggregates of a given length are equivalent, and all cyclic aggregates of a given length are likewise equivalent. Therefore, the cumulative volume fractions ϕ_{linear}(MW) and ϕ_{loop}(MW) of all the linear species and of all the cyclic species of a given molecular weight MW will be used to evaluate the impacts of the following parameters on rheological solution properties: binding energy, concentration and degree of polymerization of the single-chain building blocks, and presence or absence of "end-capping" chains (Figures 4.6–4.11).

4.4.1 Mixtures of A----A and B----B Chains Only

At the lowest level of complexity, we consider solutions of telechelics of equal molecular weights ($MW_A = MW_B = MW_p$) and equal initial volume fractions ($\phi_{Atotal} = \phi_{Btotal} = \phi_{total}/2$). In this case, the problem is reduced to understanding the association behavior as a function of MW_p, ϕ_{total}, and the energy of interaction ε. The rationale for the part of the parameter space which we investigate here is given in the Section 4.5.2.

Comparison of model results for MW_p = 10^6 g/mol (labeled 1000k in figures) at total polymer volume fraction ϕ_{total} of 1400 ppm and 800 ppm (Figures 4.6–4.7) demonstrates two important effects of total polymer concentration. First, at fixed MW_p and ε, increasing concentration results in a higher fraction of the polymer becoming involved in larger linear aggregates (compare first and second rows in Figures 4.6–4.7): the decrease in ϕ_{linear} with increasing aggregate MW is not as sharp at 1400 ppm, and the position of the peak in ϕ_{linear} vs. MW is shifted to the right at 1400 ppm for each ε (most visibly for ε =18, left column of Figure 4.7). Second, the relative partitioning of the polymer into linear rather than cyclic aggregates is insensitive to total polymer concentration ϕ_{total}.

Consider now the effect of the length of the individual chains (MW_p), by comparing results for 5 × 10^5 chains at 1400 ppm (third row, Figures 4.6–4.7) and 1 × 10^6 g/mol chains at 800 ppm (second row). These concentrations were chosen to correspond to one-fourth of the overlap concentration of the single-chains, i.e., ϕ_{total} = ¼ ϕ^* based on the respective values of MW_p. We observe that the shape of the ϕ_{linear} vs. MW curves for both these systems is nearly identical, for each value of ε investigated. On the other hand, the relative proportion of loops vs. linear chains is substantially higher for the shorter chains, due to the smaller entropic cost of cyclization for shorter loops.

Finally, the effect of the energy of association on the equilibrium distributions is very pronounced (the columns of Figures 4.6–4.7 are in ascending order by association energy). First, higher values of ε strongly increase the population of loops of all sizes, i.e., increasing ε increases the relative fraction of loops compared to linear aggregates. Second, increasing ε greatly broadens the distribution of ϕ_{linear} vs. MW, decreasing the magnitude of the peak in the distribution. At values of $\varepsilon \leq 14$, aggregates are few and the dominant components are the telechelic building block themselves. At values of $\varepsilon \geq 20$, the dominant components are cycles of low MW, but the distribution of linear supramolecules is nearly flat, meaning that very large aggregates have a significant cumulative volume fraction at equilibrium. Intermediate values of the energy of association, corresponding to $16 \leq \varepsilon \leq 18$, provide a balance of interactions strong enough to drive formation of large superchains and weak enough to accommodate a significant population with unpaired ends (i.e., linear superchains).

4.4.2 Mixtures of A----A, B----B, and A---- Chains

Important changes in the partitioning of the polymer occur as end-capping A---- chains are added to solutions of A----A and B----B telechelics. At the lowest level of complexity again, we consider solutions of polymer additives of equal molecular weight ($MW_A = MW_B = MW_{cap} = MW_p$). We consider solution compositions that maintain equal number densities of A and B endgroups, i.e., such that $\phi_{captotal} = 2(\phi_{Btotal} - \phi_{Atotal})$. Therefore, the total polymer fraction of A---- end-capping chains, $\phi_{captotal}$, must be in the range from 0 to 2/3. Define $X = \phi_{Atotal}/\phi_{Btotal}$ as the ratio of telechelics A----A to telechelics B----B; that ratio decreases from 1 to 0 as the fraction of A---- increases from 0 to 2/3.

Results obtained for solutions of $MW_p = 10^6$ g/mol at total volume fraction $\phi_{Atotal} + \phi_{Btotal} + \phi_{captotal}$ = 800 ppm (Figures 4.8–4.11) confirm that introducing end-caps favors the formation of linear species. At fixed ε, MW_p, and ϕ_{total}, the fraction of polymer involved in cycles decreases with increasing volume fraction of A---- end-caps, as expected (see top row of Figures 4.8–4.11). This is true at all values of ε and occurs simply because the presence of A---- components decreases the fraction of linear chains that *can* form loops. Note that the increase in the concentration of linear species upon addition of A---- (offsetting the decrease in ϕ_{loop}) heavily favors short, rather than long aggregates: in fact, the population of very long linear superchains is reduced by adding end-caps (decreasing X), and this was also true at all values of ε (most visible in bottom row of Figures 4.8 and 4.9). In other words, increasing the volume fraction $\phi_{captotal}$ of end-capping chains causes a narrowing of the distribution of linear aggregates, meaning that a higher fraction of polymer is involved in smaller linear supramolecules.

A striking qualitative difference between the binary (A----A + B----B) and the ternary systems is in the behavior as $\varepsilon \rightarrow \infty$. In the absence of end-capping A----, the ratio of linear to cyclic supramolecules vanishes as $\varepsilon \rightarrow \infty$ (Figure 4.7). As the free energy penalty for leaving unpaired stickers diverges, no linear chains can survive in the absence of end-caps. When end-caps are present, one is free to increase ε without extinction of linear species; instead as $\varepsilon \rightarrow \infty$ a limiting distribution is achieved (Figure 4.11) in which doubly end-capped linear species and cyclic species equilibrate in a manner that can be quantitatively controlled by the choice of the relative number of A---- single chains.

4.5 Discussion

4.5.1 Using the Model to Design Anti Misting Additives

While the model may find wide utility for diverse applications involving rheology modifiers, here we wish to identify a set of parameter values for which the equilibrium distribution of the polymer components is suitable for mist-suppression applications. The figures of merit for this application are deduced from the prior literature on ultra-long polymers, which themselves are not acceptable because turbulent flow during transport of fuel cleaves the chains and eliminates their effectiveness. As a guide to experiments to determine whether or not the efficacy of ultra-long chains and the resistance to shear degradation of associative polymers can be combined, we use the present model to guide the selection of chain lengths, association strengths, and mixture compositions that hold the greatest promise.

Chao and coworkers[8] reported that polyisobutylene chains of molecular weight ~ 5×10^6 g/mol were satisfactory mist-suppressing agents at concentrations as low as 50 ppm in kerosene. Considering that cyclic polymer chains are expected only to be as effective as linear chains of half their size, the cumulative amount of linear species of MW $\geq 5 \times 10^6$ g/mol and cycles of MW $\geq 10 \times 10^6$ g/mol should be 50 ppm or more. Given that aviation fuel is continuously circulated on the aircraft as a heat transfer fluid, the kinetics of equilibration may play a role, i.e., in practice long linear aggregates may not achieve their equilibrium distribution (refer to Section 4.5.4). If so, polymer designs and mixture compositions that maximize the *equilibrium fraction* of polymer involved in linear supramolecular aggregates in the 5–10 $\times$ 10^6 g/mol range may lead to maximal mist suppression in practice.

4.5.2 Parameter Space

By restricting the level of complexity (choosing the A----A, B----B, and A---- building blocks to be of the same molecular weight MW_p, and by requiring that A and B endgroups have equal number densities in solution), the parameter space is reduced to 4 dimensions. Within the parameter space $\{MW_p, \varepsilon, \phi_{total}, X\}$, we seek to optimize the equilibrium partitioning of the polymer for mist-control applications given the constraints of the problem.

Here we consider the bounds that are imposed on MW_p and ϕ_{total} in the context of fuel additives.

First, we should use the highest possible values of MW_p, since at fixed ε and ϕ_{total} the total fraction of polymer trapped in loops decreases monotonically with increasing MW_p. In reality the upper-bound of MW_p is limited by mechanical degradation of the polymer. Unintentional chain scission of our telechelics would result in an excess of end-capping species that would greatly reduce the size of supramolecular chains that form. Literature on shear degradation shows that flexible linear chains of less than a few million g/mol resist degradation associated with flow through pumps and turbulent pipeline flow. Therefore, we imposed $MW_p = 10^6$ g/mol as our upper bound and compared results with $MW_p = 0.5 \times 10^6$ g/mol in order to quantitate sensitivity to changes in MW_p.

Next, implementation of a polymer-based mist-control technology cannot be possible unless changes in shear viscosity of the fuel due to polymer addition are very small. Here we chose an upper bound in total volume fraction of polymer to be one-fourth of the overlap concentration of the A----A and B----B, and A---- building blocks, recognizing that supramolecular chains formed by physical associations may reach or exceed their overlap concentration. So long as the very long supramolecules remain below their particular c^*, the shear viscosity of the solution is expected to remain within permissible bounds. For the two chain lengths selected above, this constraint imposes a maximum polymer volume fraction of 800 ppm for $MW_p = 10^6$ g/mol and 1400 ppm for $MW_p = 5 \times 10^5$ g/mol. To quantify the improvements in mist control arising from increases in concentration, results for 10^6 g/mol chains at both 800 and 1400 ppm were compared.

With the above choices for MW_p and ϕ_{total}, the problem is reduced to two dimensions, ε and X, which were examined over their physically relevant ranges.

4.5.3 Implication for Mist-Control Applications

Our criterion for optimal results with regard to mist-suppressing applications corresponds to maximizing the equilibrium fraction of polymer involved in linear supramolecular aggregates in the 5–10 $\times 10^6$ g/mol range. Two key features of the distributions that satisfy this objectives are (i) favorable partitioning of the polymer into linear rather than cyclic

aggregates, and (ii) a concentration vs. molecular weight curve for linear aggregates that is narrowly distributed and centered around ~ 5×10^6 g/mol.

According to the above criteria, model results show that partitioning of the polymer into linear superchains is favored at higher values of MW_p and ϕ_{total}, as expected, but that ~ 2-fold changes in MW_p or ϕ_{total} about the ~ {10^6 g/mol, 800 ppm} upper-boundary determined by the problem constraints yield only small changes in the overall *shapes* of the ϕ_{linear}, ϕ_{loop} distributions (compare first and second rows, and first and third rows at fixed ε in Figures 4.6 and 4.7). Effects of the energy of interaction were much more pronounced. For example, a $\leq$ 15% change in ε from 14 to 16 yielded a dramatic change in the shape of the size distribution of aggregates for all values of {MW_p, ϕ_{total}} (Figure 4.6).

The strong dependence of the size distribution of linear and cyclic aggregates on energy of interactions has important implications for mist-control applications. For mixtures of A----A and B----B molecules, model predictions indicate that "good" results are only achieved in a narrow range of association energy, $16 \leq \varepsilon \leq 18$. The following two complications immediately arise. First, the preparation of telechelic chains of such length (~ 10^6 g/mol) terminated with endgroups that all bind with a precise target strength of interaction of such magnitude (> 16 kT) poses a tremendous synthetic challenge (see Section 4.5.6). Second, the strength of physical associations is strongly temperature dependent and the operating temperature range of interest for aviation fuel is very broad (-50 to +50 ^oC), so it is doubtful that any system could be designed to maintain the binding energy of the polymer endblocks within such a narrow range.

Addition of A---- end-capping chains to A----A + B----B mixtures solves the above problem, at least under equilibrium conditions. For instance, model results for 10^6 g/mol chains at ϕ_{total} = 800 ppm and X = 0.5 (Figure 4.11) show that for any value of $\varepsilon \geq 20$, the equilibrium volume fraction of linear superchains of 5×10^6 g/mol is greater than 100 ppm and that of 7×10^6 g/mol superchains is greater than 50 ppm. This means that the mist-suppression effectiveness of such a polymer solution under equilibrium conditions will be robust with respect to fluctuation in ε due to temperature variations or to variations in molecular structure of the endgroups. The model, therefore, indicates that it should be feasible to create polymers whose equilibrium distribution of aggregates provides the requisite concentration of very long supramolecular chains over a wide range of temperature.

At this point, we need to inquire whether it is reasonable to expect that equilibrium partitioning of the polymer will be found under conditions of practical import.

4.5.4 Time to Reach the Equilibrium Distribution

Earlier we explored whatever values of $\{\varepsilon, X\}$ allowed us to optimize the equilibrium distribution of polymer components. In doing so we assumed that under conditions of practical importance, equilibrium is restored as fast it is disturbed. How long does it take to reach the equilibrium partitioning of the polymer into aggregates of all sizes? Let us start by considering the lifetime of a bond. The relaxation time $\tau_0 \sim \eta b^3/kT$ of a monomer in solution of shear viscosity ~ 1 mPa.s is on the order of 10^{-10} sec, so the lifetime of a donor-acceptor physical bond $\tau_b \sim \tau_0 \exp(\varepsilon)$ is on the order of 0.001–10 sec for ε = 17–25. Therefore, even if we assumed that equilibrium could be reached with a mere 10^3 bond breaking and bond forming events, for endgroups associating with energy 20–25kT, that time is on the order of $1–10^4$ s. Consider now that processes such as recirculation of the fuel within an aircraft are expected to breakup polymer aggregates down to individual components at intervals of a few minutes during, for example, passage through pumps. Given the level of uncertainty in our calculations, experimentation is required to reach a definite conclusion about whether or not solutions of A----A plus B----B plus A---- polymer chains reassociate into large superchains sufficiently rapidly to be used as mist-suppressing agents for aviation fuel.

4.5.5 From Telechelics to Heterotelechelics

What experiments do the model results motivate us to conduct? We found that ternary mixtures of A----A, B----B, and A---- chains in dilute solutions deserve the effort required to synthesize the polymer. Unfortunately, they suffer to some extent from the same problems as mixtures of A----A and B----B chains only (whose binary mixtures do not appear to be viable candidates for mist-suppressing applications): (i) to provide 50 ppm of superchains > 5×10^6 g/mol, the overall polymer concentration must be several hundred ppm because a lot of polymer is "lost" in useless small cycles and small linear aggregates, and (ii) the reassembly of superchains takes time, and the longer the superchain the longer it takes for its population to build up to its equilibrium value.

The above insight suggests that a better alternative would involve the design of a polymer system for which loops are prohibited and associations would result in the systematic

formation of well-defined linear chains. An example of such a design is shown in Scheme 4.3. It involves two sets of specific interactions, such that A endgroups interact only with B endgroups, and C endgroups likewise only with D endgroups. The molecules in Scheme 4.3 are designed such that for a stoichiometric blend of the building blocks and at high enough binding affinity of the A+B and C+D associations, nearly all the polymer chains should assemble into pentamers (in 4 bond-forming events only) even at arbitrarily low polymer volume fraction ϕ_{total}. As a result, satisfactory mist suppression could be achieved with < 100 ppm of A----A, B----C, and D---- chains of size $MW = 10^6$ g/mol.

4.5.6 Nature of the Endgroups

We now address an important synthetic challenge. What chemical moieties might we use at the chain ends to generate association energies in the 17–25kT range? Let A and B refer to the small molecules corresponding to these endgroups. We first inquire what equilibrium constant of association K_{ass} the above association energies correspond to. For the association reaction of the free-endgroups A + B → AB, our model predictions are:

$$\frac{\phi_{AB}}{M_{AB}} = \left(\frac{\phi_A}{M_A}\right)\left(\frac{\phi_B}{M_B}\right)\exp\left[-\frac{1}{kT}\left(\mu_{AB}^0 - \mu_A^0 - \mu_B^0\right)\right] = \exp(\varepsilon)\,. \tag{4.32}$$

For small molecules in dilute solution, this expression is consistent with the equilibrium condition for ideal solutions (Raoult's law), $x_{AB}/x_A x_B = \exp[-(\mu_{AB}^0 - \mu_A^0 - \mu_B^0)]$, where x is mole fraction. It follows from Equation 4.32 that $K_{ass} \equiv C_{AB}/C_A C_B = \upsilon_s \exp(\varepsilon)$, where C is molar concentration and υ_s is the molar volume of the solvent. Thus, achieving binding energies of the endgroups in the range of ε = 17–25 corresponds to association constants K_{ass} on the order of 10^7 to 10^{10} M^{-1}!

Although interacting chemical structures of binding constants up to 10^6 M^{-1} are known (Figure 4.12), the synthetic challenge of preparing telechelic polymer chains of size 10^6 g/mol with well-defined endgroups of binding constants ~ 10^7 to 10^{10} M^{-1} is daunting. In addition to the challenge of finding a suitable donor-acceptor pair, synthesis of telechelics becomes increasingly more difficult with increasing size. Furthermore, the possible poisoning of the endgroups (which would be present at < ppb levels in dilute polymer solutions) by minute amounts of acids, bases, metals etc… present in the solvent, thereby rendering the polymer ineffective, is an important concern.

A worthwhile alternative involves the use of short polymer endblocks featuring an arbitrary number of donor-acceptor type functional groups. For example, synthesis of 10^6 g/mol polymer chains endcapped with 1,2-PB endblocks of a few thousands g/mol would enable the preparation of associating polymer of tunable binding affinities by post-polymerization functionalization of the 1,2-PB. This strategy would provide more flexibility in the choice of binding energy and also facilitate fast and effective optimization of material properties via rapid adjustments in the number and the identity of the functional side-groups.

4.6 Conclusions

In this chapter we developed a model to understand the self-assembling behavior of polymer chains designed to overcome the effect of chain collapse (refer to Chapters 2 and 3) by clustering stickers at the ends of polymer chains. We showed that symmetric linear chains displaying strongly associating endgroups (A----A and B----B binary mixtures) suffer instead from loop formation, which traps large amounts of the polymer into small cyclic aggregates with low mist-control properties. We found that more favorable equilibrium distributions for the purpose of mist-control applications can be achieved by addition of end-capping A---- chains. Future work might involve experimentation to determine whether ternary mixtures of A----A, B----B, and A---- polymer chains that associate end-to-end with binding energies > 10^7 M^{-1} can build up large superchains sufficiently rapidly to be used as mist-suppressing agents for aviation fuel. This presents a synthetic challenge which we addressed above. We reasoned that functional endgroups would best be achieved by synthesis of short polymer endblocks bearing a suitable number of selected functional groups (hydrogen bond donor and acceptor pairs, for instance).

Insight generated from the present model also suggests the design of end-to-end associating molecules which cannot form loops. Breaking symmetry to enable the exclusive formation of large linear supramolecules from self-assembly of end-functionalized polymer chains (Scheme 4.3) requires synthesis of polymer molecules featuring several orthogonal (i.e., non-interacting) pairs of complementary (i.e., donor-acceptor) endgroups. Preparation of such materials required the development of new synthetic tools: in the next chapter we present straightforward and rapid protocols for the preparation of functional polymer materials of controlled architecture and functionality.

4.7 Figures and Schemes

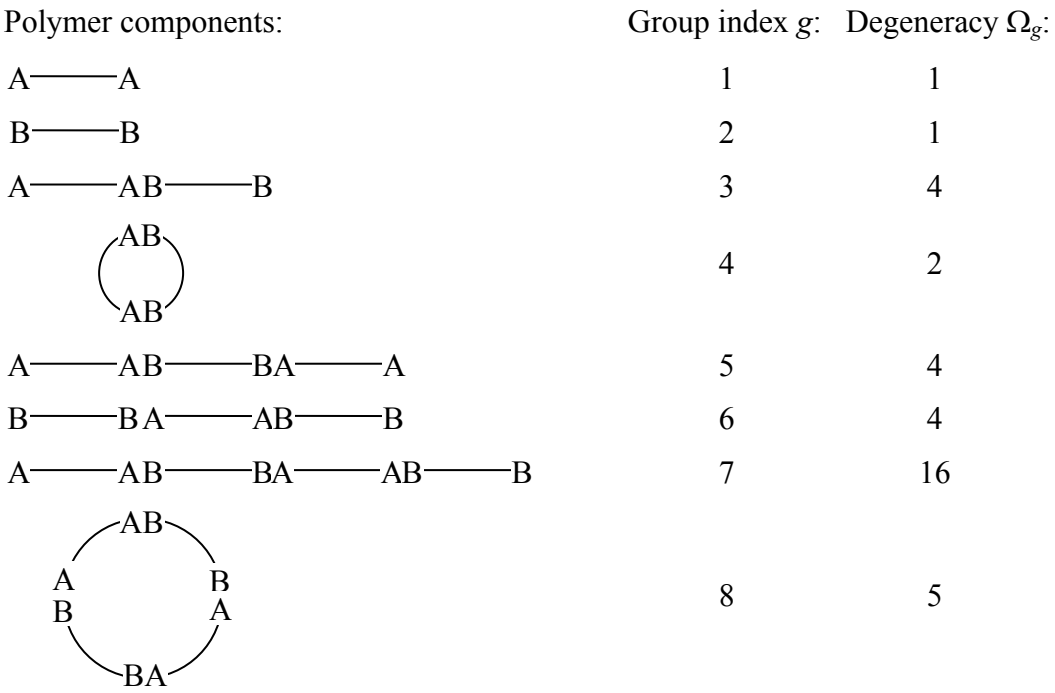

Figure 4.1 Grouping of polymer components, where A and B generically refer to A_1 or A_2 and B_1 or B_2 endgroups. Each group is composed of all the different possible aggregates obtained by the assembly of the A_1----A_2 and B_1----B_2 building blocks. For example, group 3 is composed of the following 4 distinct aggregates: A_1----A_2B_1----B_2, A_1----A_2B_2----B_1, A_2----A_1B_1----B_2, and A_2----A_1B_2----B_1.

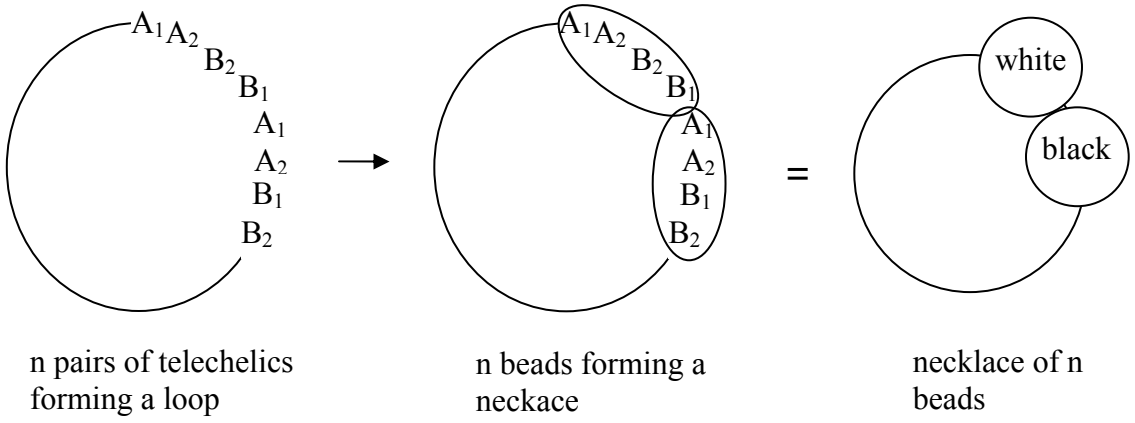

Figure 4.2 Mapping of polymer loops into necklaces of 4 colors. The 4 colors correspond to: $A_1A_2B_1B_2$, $A_1A_2B_2B_1$, $A_2A_1B_1B_2$, $A_2A_1B_2B_1$. For example, we can choose $A_1A_2B_1B_2$ = black, $A_1A_2B_2B_1$ = white, $A_2A_1B_1B_2$ = blue, and $A_2A_1B_2B_1$ = green.

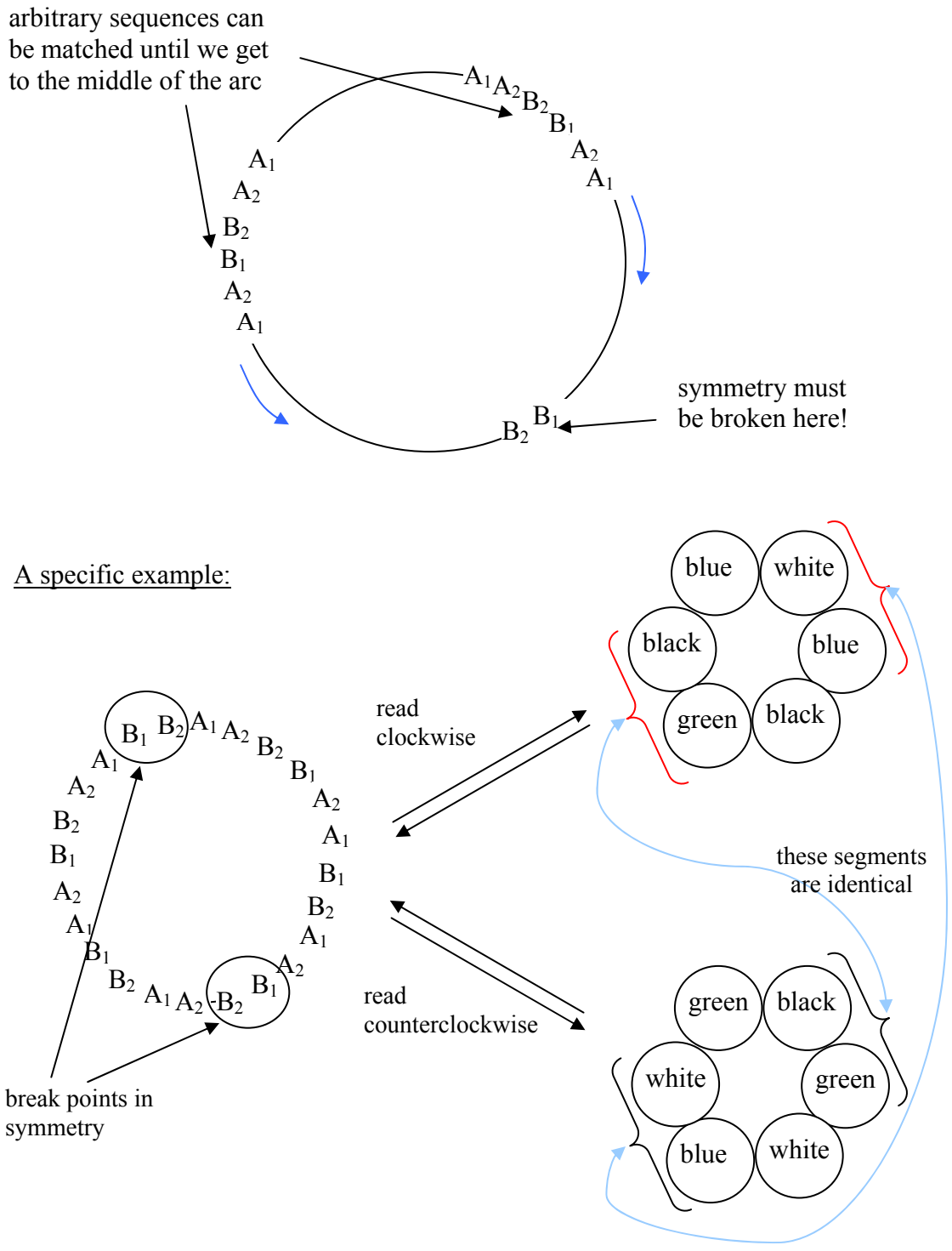

Figure 4.3 We cannot arbitrarily create a loop that "reads" the same clockwise and counterclockwise. Therefore, every loop maps into exactly two distinct necklaces. (Color assignments are given in Figure 4.2.)

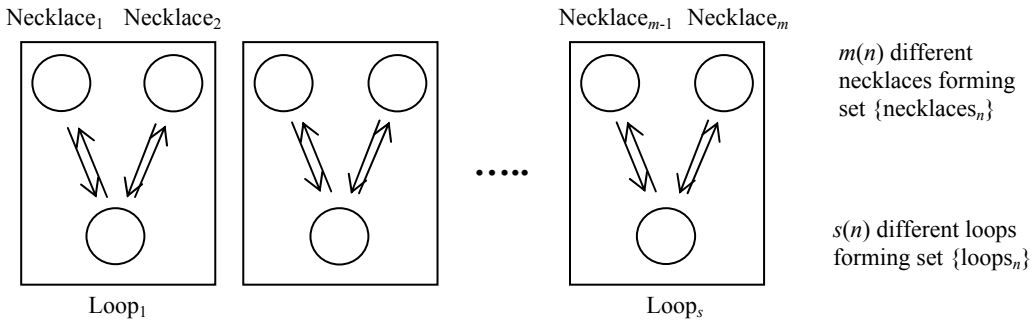

Figure 4.4 There are twice as many distinct necklaces as there are distinct loops.

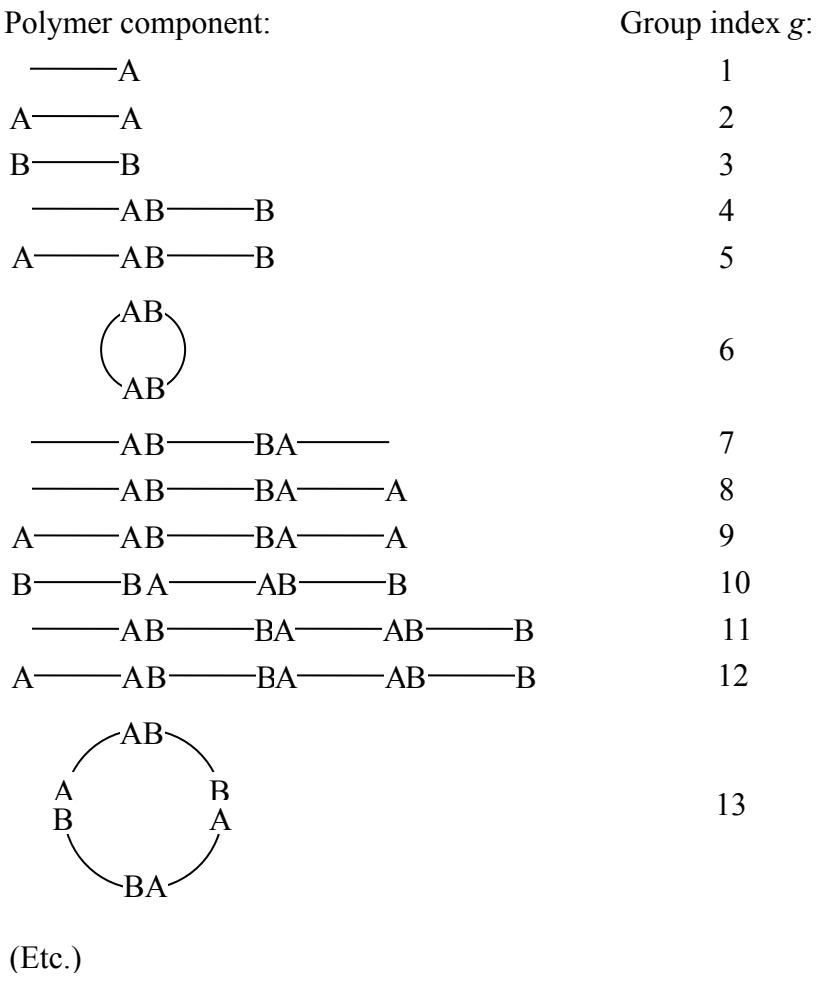

Figure 4.5 Grouping of polymer components in the presence of A---- end-capping chains. Each group is composed of all the different possible aggregates obtained by the assembly of the A_1----A_2, B_1----B_2, and A---- building blocks, as before (Figure 4.1).

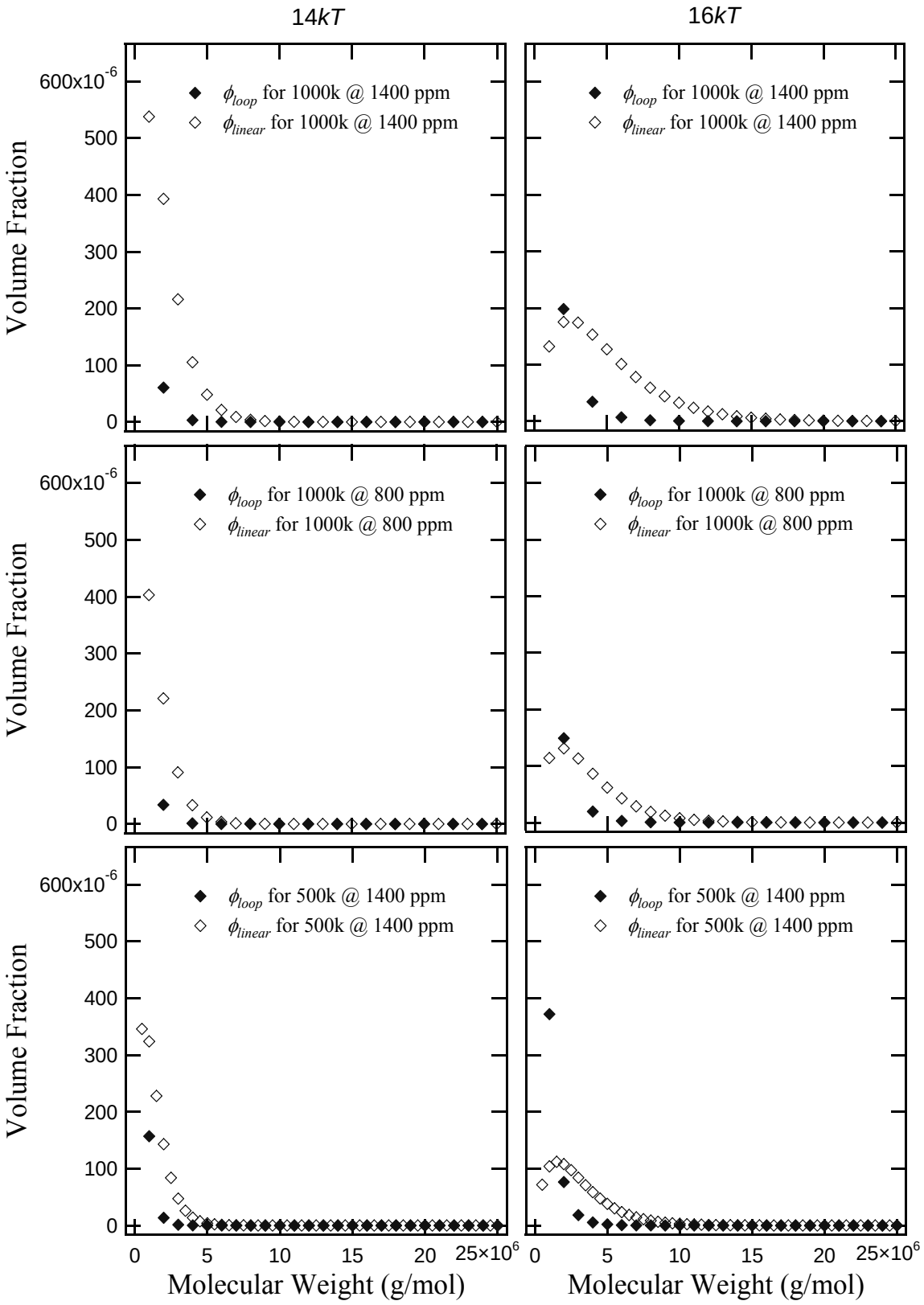

Figure 4.6 Model predictions for strength of interaction $\varepsilon kT = 14kT$ (left) and $\varepsilon kT = 16kT$ (right).

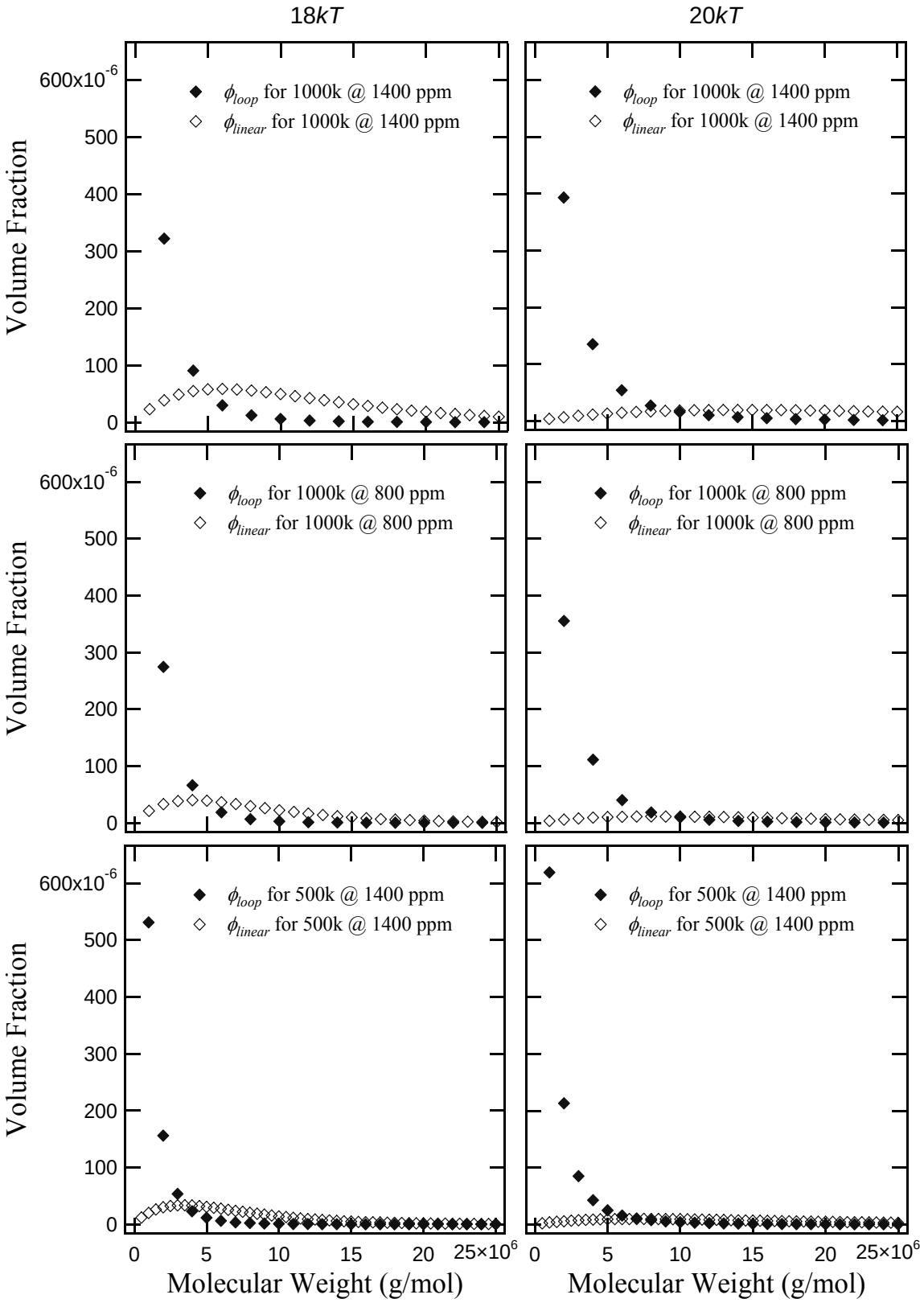

Figure 4.7 Model predictions for strength of interaction $\varepsilon kT = 18kT$ (left) and $\varepsilon kT = 20kT$ (right).

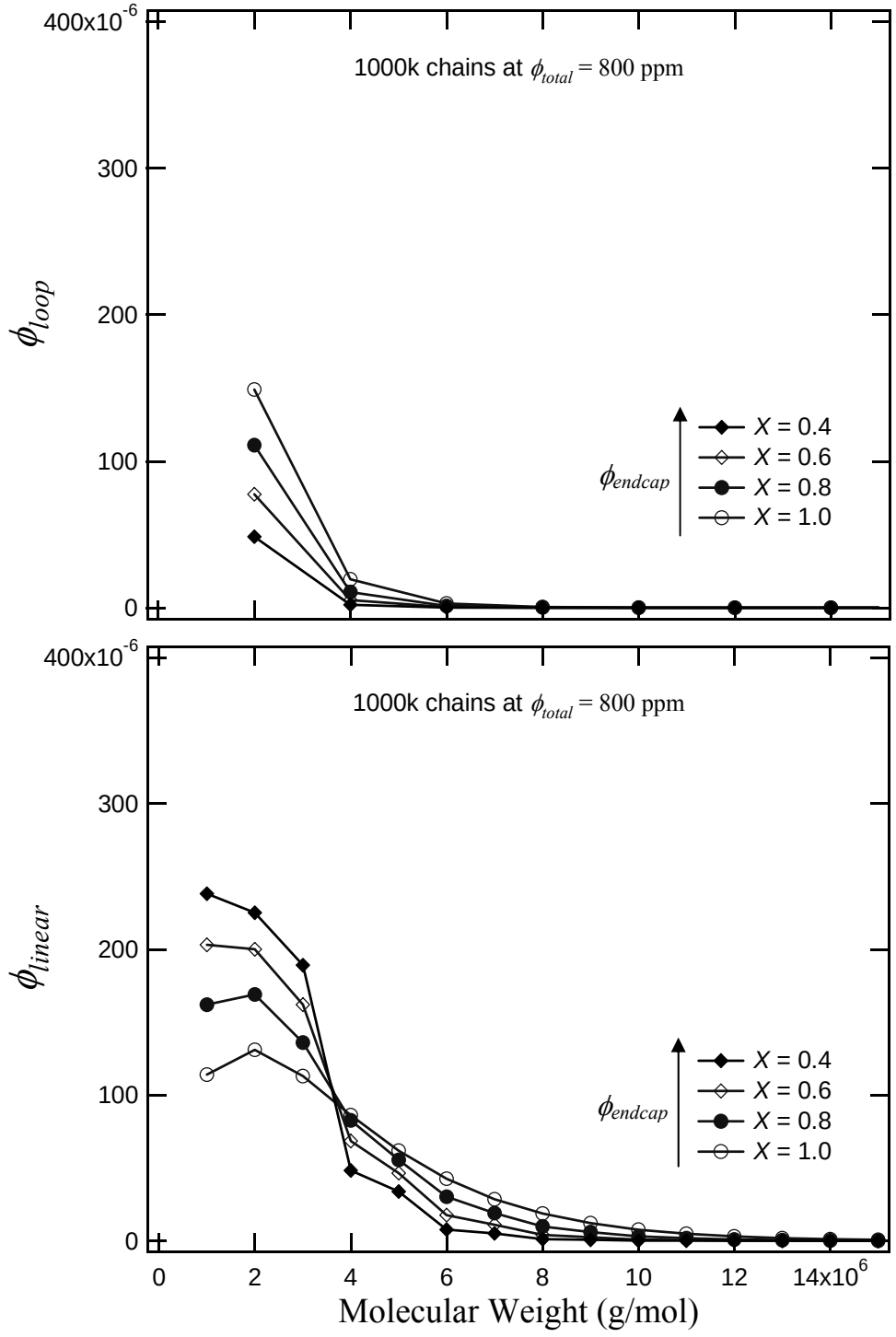

Figure 4.8 Model predictions in the presence of end-capped chains, when $\varepsilon kT = 16kT$.

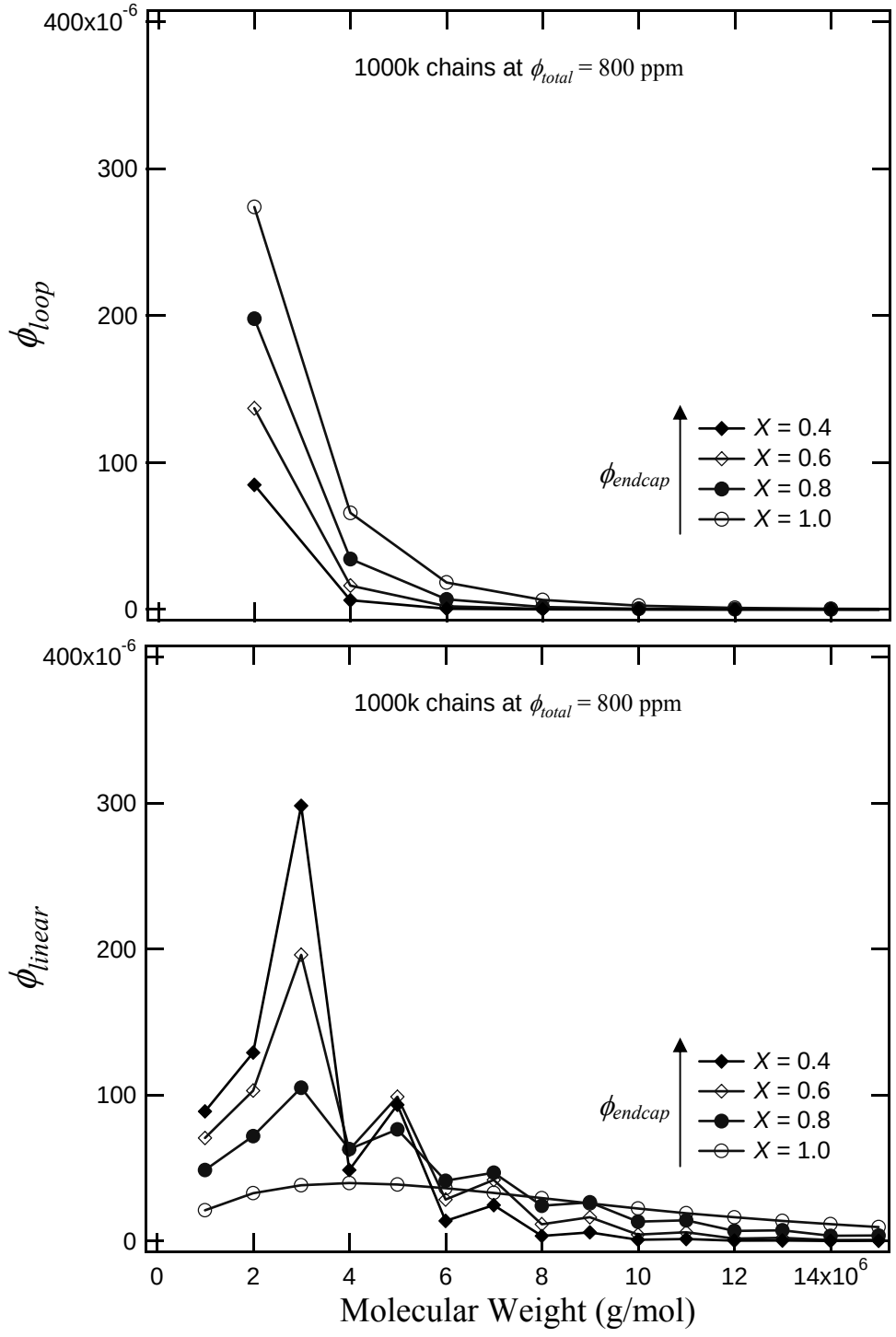

Figure 4.9 Model predictions in the presence of end-capped chains, when $\varepsilon kT = 18kT$.

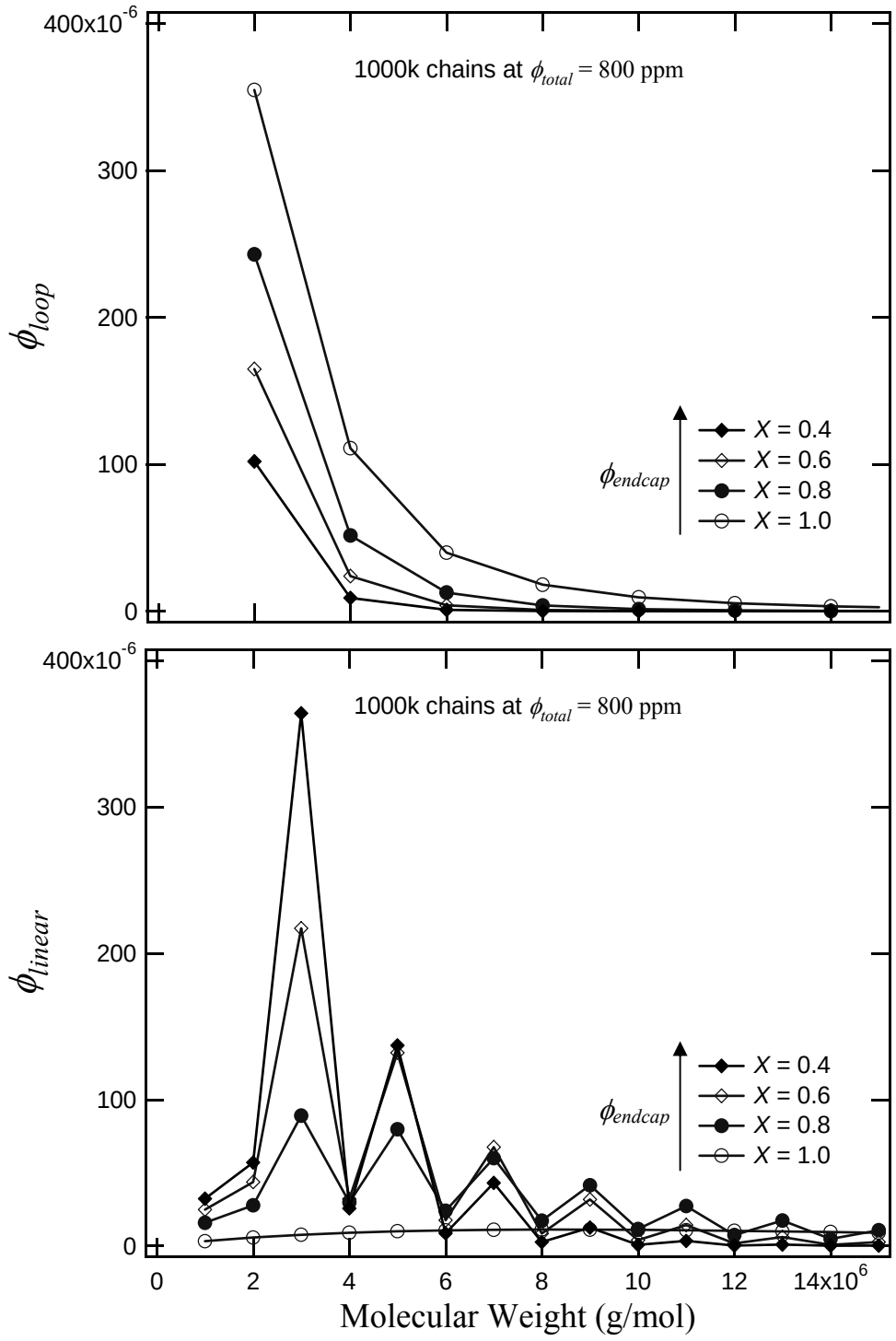

Figure 4.10 Model predictions in the presence of end-capped chains, when $\varepsilon kT = 20kT$.

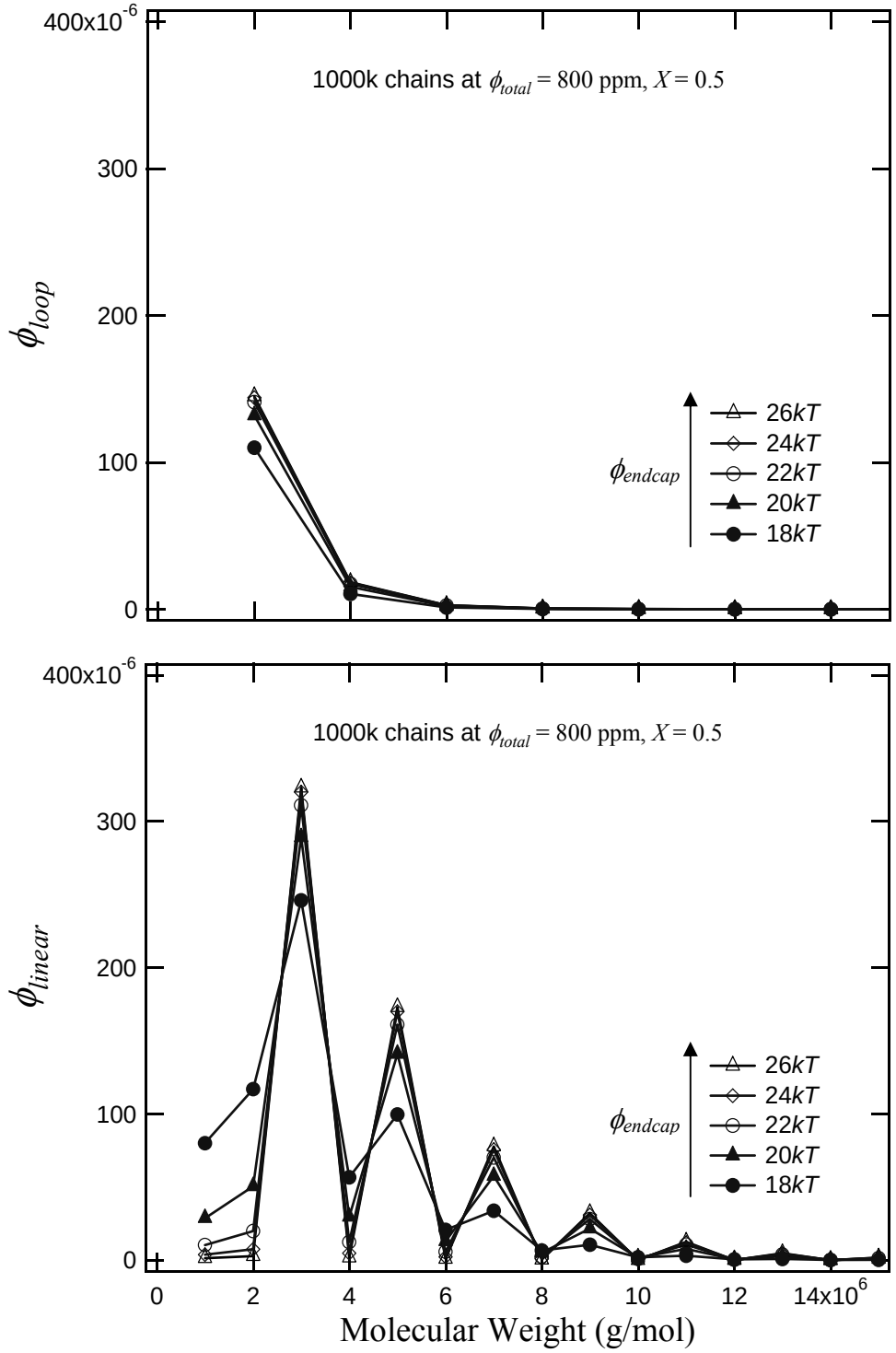

Figure 4.11 Limiting equilibrium distribution (as $\varepsilon \rightarrow \infty$) obtained in the presence of end-capping A---- polymer chains.

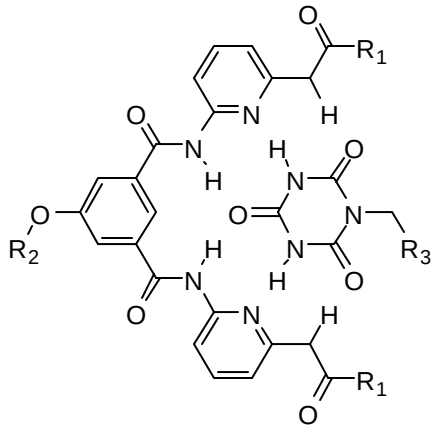

Figure 4.12 Sextuple hydrogen-bonding motifs derived from nucleobase structures, of binding constants ~ 10^6 M^{-1} in organic solvents of low polarity.[9, 10]

Scheme 4.1 Molecular Design for Self-Assembly of Difunctional Polymeric Building Blocks into Larger Linear Chains via Physical Interactions

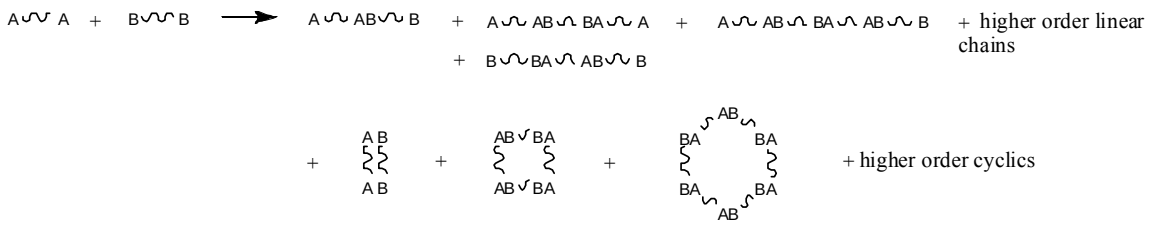

Scheme 4.2 Contact Probabilities and Equilibria

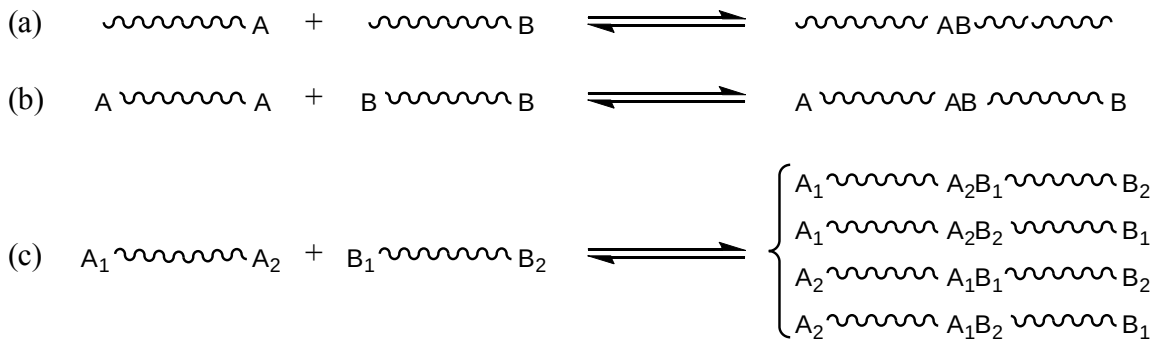

Scheme 4.3 Molecular Design Aimed at the Exclusive Formation of Well-Defined Supramolecular Linear Chains

4.8 References and Notes

1. Compare with lattice model of Goldstein (Goldstein, R. E., Model for Phase-Equilibria in Micellar Solutions of Nonionic Surfactants. *Journal of Chemical Physics* **1986,** 84, (6), 3367–3378).

2. Hill, T. L., In *An Introduction to Statistical Thermodynamics*, Dover Publications: 1986; pp. 402–404.

3. Rubinstein, M.; Colby, R. H., In *Polymer Physics*, Oxford: 2003; p. 70.

4. Rubinstein, M.; Colby, R. H., In *Polymer Physics*, Oxford: 2003; pp. 121–122.

5. van Lint, J. H.; Wilson, R. M., In *A Course in Combinatorics*, Cambridge University Press: 2001; pp. 522–525.

6. Rubinstein, M.; Colby, R. H., In *Polymer Physics*, Oxford: 2003; p. 53, Table 2.1.

7. Obtained from viscosity measurements of 580 kg/mol polyisoprene chains, of polydispersity index 1.22, in Jet-A solvent, by rearrangement of the scaling relation $\phi^* \approx (b^3/v)^{6\nu-3}N^{1-3\nu}$ (Rubinstein, M.; Colby, R. H., *Polymer Physics*. Oxford: 2003, Equation 5.19, p. 176) using swelling exponent $\nu \approx 0.588$ and overlap concentration $\phi^* \cong 0.0049$. The number of Kuhn monomers N was estimated using $MW_K = 113$, and the overlap concentration was determined according to the criterion $[\eta]\phi^* \cong 1$.

8. Chao, K. K.; Child, C. A.; Grens, E. A.; Williams, M. C., Antimisting action of polymeric additives in jet fuels. *AICHE Journal* **1984,** 30, (1), 111–120.

9. Binder, W. H.; Kunz, M. J.; Kluger, C.; Hayn, G.; Saf, R., Synthesis and analysis of telechelic polyisobutylenes for hydrogen-bonded supramolecular pseudo-block copolymers. *Macromolecules* **2004,** 37, (5), 1749–1759.

10. Kolomiets, E.; Buhler, E.; Candau, S. J.; Lehn, J. M., Structure and properties of supramolecular polymers generated from heterocomplementary monomers linked through sextuple hydrogen-bonding arrays. *Macromolecules* **2006,** 39, (3), 1173–1181.